Theoretical and experimental study of fundamental differences in the noise suppression of high-speed SOA-based all-optical switches

Mads L. Nielsen and Jesper Mørk

Research Center COM, Technical University of Denmark, Bldg. 345v, DK-2800 Kgs. Lyngby, Denmark
mln@com.dtu.dk

Rei Suzuki, Jun Sakaguchi, and Yoshiyasu Ueno

Graduate School of Electronic Engineering, University of Electro-Communications, 1-5-1 Chofugaoka, Chofu, Tokyo, 182-8585, Japan

Abstract: We identify a fundamental difference between the ASE noise filtering properties of different all-optical SOA-based switch configurations, and divide the switches into two classes. An in-band ASE suppression ratio quantifying the difference is derived theoretically and the impact of the ASE filtering on the optical spectrum is verified experimentally using a hybrid DISC setup. ASE power suppression of around 3 dB over the total signal bandwidth is demonstrated.

©2005 Optical Society of America

OCIS codes: (060.2330) Fiber optics communications; (250.5980) Semiconductor optical amplifiers

References and links

1. J. Leuthold, B. Mikkelsen, G. Raybon, C. H. Joyner, J. L. Pleumeekers, B. I. Miller, K. Dreyer, R. Behringer, "All-optical Wavelength Conversion between 10 and 100 Gb/s with SOA Delayed-interference Configuration", Opt. Quantum Electron. **33**, 939 (2001)
2. Y. Ueno, S. Nakamura, K. Tajima, "Nonlinear Phase Shifts induced by Semiconductor Optical Amplifiers with Control Pulses at Repetition Frequencies in the 40-160 GHz Range for Use in Ultrahigh-Speed All-optical Signal Processing," J. Opt. Soc. Am. B **19**, 2573 (2002)
3. J. Mørk, F. Öhman, S. Bischoff, "Analytical Expression for the Bit-Error-Rate of Cascaded All-optical Regenerators," Photonics Technol. Lett. **15**, 1479 (2003)
4. M. L. Nielsen, J. Mørk, "Increasing the Modulation Bandwidth of Semiconductor Optical Amplifier based Switches using Optical Filtering," J. Opt. Soc. Am. B. **21**, 1606 (2004)
5. N. S. Patel, K. L. Hall, K. A. Rauschenbach, "40-Gbit/s cascadable all-optical logic with an ultrafast nonlinear interferometer," Optics Lett. **21**, 1466 (1996)
6. J. P. Sokoloff, P. R. Prucnal, I. Glesk, M. Kane, "A terahertz optical asymmetric demultiplexer (TOAD)," Photonics Technol. Lett. **5**, 787 (1993)
7. R. J. Manning, A. Antonopolous, R. Le Roux, A. E. Kelly, "Experimental measurement of nonlinear polarisation rotation in semiconductor optical amplifiers," Electron. Lett. **37**, 229 (2001)

1. Introduction

All-optical switches for signal regeneration and processing based on cross-phase modulation (XPM) in semiconductor optical amplifiers (SOA) have demonstrated great potential in terms of high switching speed, small footprint, and low power consumption [1,2]. An inherent property of SOA-based switches is the addition of amplified spontaneous emission (ASE) noise to the switched signal, which degrades the signal quality and ultimately the receiver sensitivity. In a chain of regenerators, the amount of ASE added by the SOA(s) of each regenerator influences the requirements to the following regenerators [3]. Specifically, an increased ASE emission puts an increasingly strict requirement on the nonlinearity of the regenerator transfer function, which is very challenging at high bitrates.

#7331 - $15.00 USD Received 3 May 2005; revised 13 June 2005; accepted 19 June 2005

In this paper, we report on a fundamental difference between the amounts of ASE emitted from two classes of all-optical, interferometric, SOA-based switches. In such switches, the data signal cross-phase modulates a probe signal through refractive index changes in an SOA, and the transmittance of the probe signal is governed by the resulting interference condition at the output. By operation in the so-called differential-mode of operation, these switches may be operated at speeds far exceeding the carrier density modulation bandwidth [2,4]. The first class, exemplified by the delayed-interference signal converter (DISC) [1,2,4], Fig. 1(a), contains switches consisting of a single SOA and an external interferometer acting as a filter, while the second class, exemplified by the SOA-based Mach-Zehnder interferometer (MZI), Fig. 1(b), contains SOAs in the arms of the interferometer. Both devices have been monolithically integrated and are thus considered prime candidates for implementation of all-optical switching in networks [1,2]. The ASE emitted from both configurations is analyzed theoretically and the findings are verified experimentally.

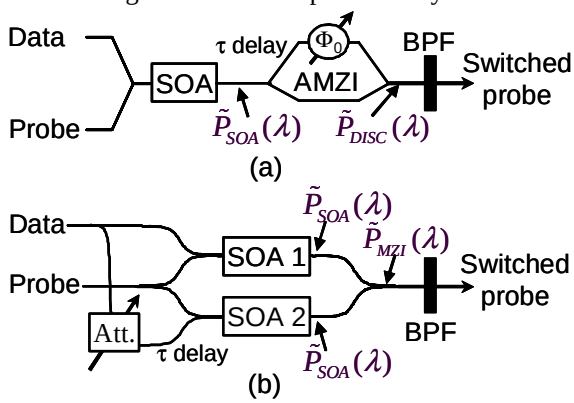

Fig. 1. Schematics of (a) the DISC configuration and (b) the SOA-based MZI configuration.

2. Theoretical description

The SOAs in the switches provide the phase modulation that facilitates switching, but also act as noise sources. As indicated in Fig. 1 the ASE spectral power density after each SOA is denoted $\tilde{P}_{SOA}(\lambda)$, whereas the corresponding densities after the DISC and MZI are referred to as $\tilde{P}_{DISC}(\lambda)$ and $\tilde{P}_{MZI}(\lambda)$, respectively. At bitrates below the carrier density modulation bandwidth, cross-gain modulation (XGM) is efficient and $\tilde{P}_{SOA}(\lambda)$ will be modulated according to the data pattern. However, at high bitrates, above the carrier modulation bandwidth, where it is necessary to employ the differential-mode of operation to obtain switching, it is reasonable to neglect XGM [4]. Consequently, in this regime the ASE spectral power density $\tilde{P}_{SOA}(\lambda)$ can be regarded as independent of whether a logic "1" or logic "0" is received. For the MZI, the two SOAs represent two mutually incoherent noise sources, which means that any interference between the two will average out. Consequently, taking the 50/50 coupler into account, the ASE spectral density at the output becomes $\tilde{P}_{MZI}(\lambda) = ½\tilde{P}_{SOA}(\lambda) + ½\tilde{P}_{SOA}(\lambda) = \tilde{P}_{SOA}(\lambda)$. For the DISC, the ASE spectral density at the output of the asymmetric MZI (AMZI) filter can be described as $\tilde{P}_{DISC}(\lambda) = \tilde{P}_{SOA}(\lambda)\left|H_{AMZ}(\lambda)\right|^2$, where

$$\left|H_{AMZ}(\lambda)\right|^2 = \frac{1}{2}\left[1+\cos(-2\pi\frac{\lambda-\lambda_P}{\Delta\lambda_\tau}+\Phi_0)\right] \tag{1}$$

#7331 - $15.00 USD Received 3 May 2005; revised 13 June 2005; accepted 19 June 2005
(C) 2005 OSA

is the sinusoidal power transfer function of the AMZI filter [4], here assumed to be polarization independent. The parameters Φ_0 and $\Delta\lambda_\tau = \lambda_P^2/(c\tau)$ are the phase bias and free-spectral range of the AMZI, respectively, where λ_P is the probe wavelength. Fig. 2 shows the normalized spectral density of the ASE at the output of the SOA (solid line), which is assumed wavelength independent within the considered bandwidth, and the power transfer function $|H_{AMZ}(\lambda)|^2$ (dashed curve) for a realistic phase bias of $\Phi_0 = 0.90\pi$. In practice, Φ_0 must be close to π to obtain a good extinction ratio of the switched pulses [1, 2, 4]. This implies that the notch of the transfer function is close to the carrier wavelength λ_P of the probe. As a consequence, the fringe pattern imposed by the AMZI on the ASE spectral density from the SOA, effectively suppresses ASE noise *inside* the signal bandwidth.

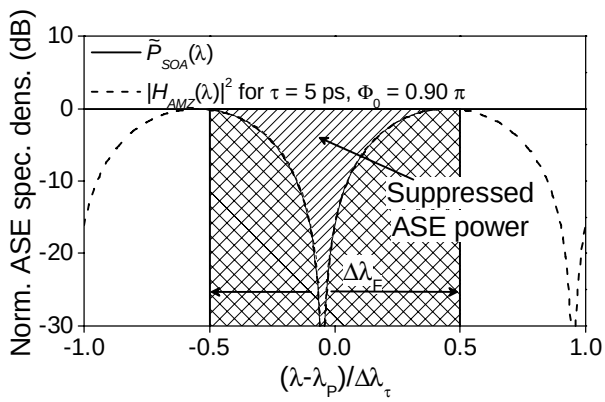

Fig. 2. Normalized ASE power spectral density of SOA output (solid) and AMZI power transfer function (dashed) for τ=5 ps and Φ_0=0.90π. Single-hatched area represents ASE power suppressed by AMZI.

The total ASE power emitted from the two switches is obtained by integrating $\tilde{P}_{DISC}(\lambda)$ and $\tilde{P}_{MZI}(\lambda)$ over the bandwidth $\Delta\lambda_F$ of the system, which may be considered given by the bandwidth of the output band pass filter (BPF) shown in Fig. 1. The ASE spectral density $\tilde{P}_{SOA}(\lambda)$ is assumed polarization independent, the validity of which is verified experimentally below. The ASE power emitted from the MZI is given by $P_{ASE}^{MZI} = \tilde{P}_{SOA}(\lambda_P)\Delta\lambda_F$. For $\Delta\lambda_F = \Delta\lambda_\tau$, P_{ASE}^{MZI} can be identified in Fig. 2 as the area of the central rectangle between ±1/2, i.e., the sum of the single and double-hatched areas. Analogously, the ASE power P_{ASE}^{DISC} emitted from the DISC is identified as the double-hatched area, and the suppressed ASE power is given by the single-hatched area. It should be stressed that the transfer function in eq. (1), experienced by the probe as well as the ASE, only depends on the differential delay τ and the phase bias Φ_0, and is thus *independent* of the phase modulation imposed by the data signal. Thus, the ASE power transmitted by the DISC during reception of a logic "0" or logic "1" is identical, and equal to the double-hatched area in Fig. 2.

P_{ASE}^{DISC} can be evaluated analytically and will be stated in terms of the *in-band ASE suppression ratio* $IBSR = P_{ASE}^{MZI} / P_{ASE}^{DISC}$, which is a measure of the ASE reduction obtained from the DISC compared to the MZI:

$$IBSR^{-1} = \frac{1}{2}\left[1 + \cos(\Phi_0)\,\mathrm{sinc}\left(\frac{\pi\Delta\lambda_F}{\Delta\lambda_\tau}\right)\right] \tag{2}$$

#7331 - $15.00 USD Received 3 May 2005; revised 13 June 2005; accepted 19 June 2005
(C) 2005 OSA

Here, the $\mathrm{sinc}(\cdot)$ function is defined as $\sin(\cdot)/(\cdot)$. Both P_{ASE}^{MZI} and P_{ASE}^{DISC} may be reduced by a factor of 2 by inserting a polarizer at the output of the switches, aligned to the polarization state of the probe, thereby eliminating the ASE power in the orthogonal polarization. However, this has no impact on the *IBSR*. According to eq. (2), *IBSR* depends strongly on the system bandwidth $\Delta\lambda_F$, and for narrow filtering ($\Delta\lambda_F \rightarrow 0$), *IBSR* goes to infinity, corresponding to a very large in-band ASE suppression. However, this noise suppression comes at the price of pulse broadening for the switched signal, which may or may not be acceptable, depending on the application. For $\Delta\lambda_F = \Delta\lambda_\tau$, as illustrated in Fig. 2, the BPF has negligible impact on the pulse width, and according to Eq. (2), this corresponds to $IBSR = 2$. Thus, under the assumptions made in this section, the DISC suppresses the switched in-band ASE power by a factor ≥2 compared to the MZI.

As mentioned, the DISC and MZI are representatives of two broader classes of optical switches. The ultra fast nonlinear interferometer (UNI) is identical to the DISC, except for an additional AMZI at the SOA input, which makes it applicable to 3R regeneration and logic functionalities [2,5]. However, at the output side of the SOA the UNI and DISC are identical, and thus provide the same in-band suppression of the ASE emitted by the SOA. Other filters with notch characteristic have the same impact on the ASE suppression, but in order to properly convert the phase modulation of the probe into amplitude modulation, the filter phase response must have a discontinuity [4]. The other class contains interferometric switches for which the interfering ASE components stem from mutually incoherent noise sources, such as the MZI illustrated in Fig. 1(b) and the SOA-based Michelson interferometer. A Sagnac interferometer with a single SOA placed asymmetrically in the loop realizes a differential-mode switch referred to as a terahertz optical asymmetric demultiplexer (TOAD) [6]. In this configuration the ASE spectral components interfering at the output port stem from different facets of the SOA, which make them mutually incoherent. Consequently, *no* fringe pattern – or in-band ASE suppression - will be observed at the output of a TOAD switch.

3. Experimental results

The experimental verification is based on measurements on a hybrid DISC setup, where different paths for orthogonal polarization components constitute the arms of the AMZI. The differential delay of τ is obtained using a birefringent calcite crystal. Details of this "inline" DISC implementation are given in [2], and will only be briefly discussed here.

The setup is illustrated in Fig. 3: a mode-locked fiber ring laser (ML-FRL) emits a 12.5 GHz train of 2 ps wide pulses at 1555 nm. This pulse train is passively multiplexed to 25 GHz in a fiber interleaver and combined with a continuous wave (CW) probe signal at 1548.5 nm from a distributed feedback laser diode (DFB-LD).

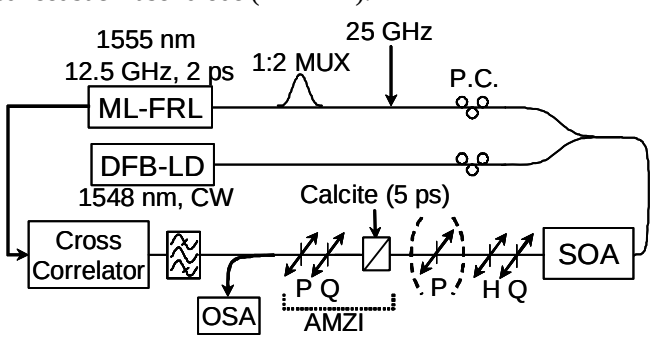

Fig. 3. Experimental setup: Inline implementation of DISC

The polarization state of both signals is aligned to one of the principal axes of the SOA using polarization controllers (P.C.). This state will be referred to as TE without any loss of generality. Using a quarter (Q) and half-wave plate (H), the polarization of the probe signal at

#7331 - $15.00 USD Received 3 May 2005; revised 13 June 2005; accepted 19 June 2005
(C) 2005 OSA

the SOA output is aligned to a linear state 45° off the principle axes of a rotatable calcite crystal with a differential delay of $\tau = 5$ ps. An optional polarizer (P) aligned to the probe is indicated in the dashed parentheses. At the output, a quarter-wave plate and polarizer constitute the phase bias Φ_0. The optical spectrum is monitored on an optical spectrum analyzer (OSA) and the waveform of the switched probe signal is observed through cross correlation with the 2 ps wide control pulses from the ML-FRL.

The sinusoidal fringe pattern in the ASE spectrum predicted by Eq. (1) is verified experimentally by including the polarizer at the AMZI input, turning the input signals off, and observing the impact of the AMZI on the ASE spectrum emitted from the SOA. Figure 4(a) shows the ASE spectrum at the DISC output, obtained for a bias current of 150 mA for both TE and TM polarized ASE at the AMZI input, shown in solid and dashed curves, respectively. The spectra are observed to be shifted from each other by $\Delta\lambda_\tau / 2$, which is a consequence of TE and TM components at the same wavelength being represented by diametrically opposite points on the Poincaré sphere. Specifically, at wavelengths for which the TE component is linearly polarized and aligned to the output polarizer for full transmittance, the TM component is orthogonal to the polarizer, and thus suppressed.

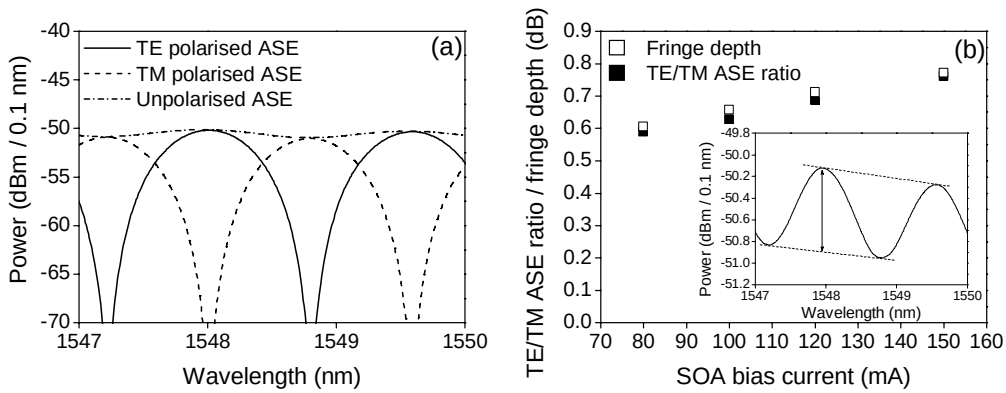

Fig. 4. (a) ASE spectra (resolution: 0.1 nm) at DISC output for TE/TM polarized ASE (solid/dashed), and for unpolarized ASE (dash-dotted). (b) Comparison of TE/TM ASE ratio (black squares) and ASE spectral fringe depth (white squares). Inset: detail of spectral fringe for I = 150 mA.

Figure 4 (a) also shows the spectrum for unpolarized ASE at the input of the inline AMZI (dash-dotted curve), corresponding to removing the polarizer. This spectrum is the sum of the spectra for TE and TM, and a slight spectral modulation is observed, which is due to the polarization dependent modal gain of the SOA. The modulation depth can be shown to be *equal* to the ratio of ASE power emitted in the TE and TM polarization states by the following considerations: Let us define $\tilde{P}_{ASE}^{TE}(\lambda) = r\tilde{P}_{SOA}(\lambda)$ and $\tilde{P}_{ASE}^{TM}(\lambda) = (1-r)\tilde{P}_{SOA}(\lambda)$ as the spectral power densities of ASE emitted from the SOA in the TE and TM states, where *r* is the fraction of ASE power emitted as TE. If the AMZI transfer function for the TE polarized ASE, $\left|H_{AMZ}^{TE}(\lambda)\right|^2$, is described by Eq. (1), the corresponding transfer function for the TM polarized components, $\left|H_{AMZ}^{TM}(\lambda)\right|^2$, is obtained by replacing Φ_0 with $\Phi_0 + \pi$ in eq. (1). The total ASE noise spectral density at the output of the inline AMZI, here denoted by the superscript "CQP", can thus be described as

#7331 - $15.00 USD Received 3 May 2005; revised 13 June 2005; accepted 19 June 2005
(C) 2005 OSA

$$\tilde{P}_{DISC}^{CQP}(\lambda) = \tilde{P}_{ASE}^{TE}(\lambda)\left|H_{AMZ}^{TE}(\lambda)\right|^2 + \tilde{P}_{ASE}^{TM}(\lambda)\left|H_{AMZ}^{TM}(\lambda)\right|^2$$
$$= \frac{\tilde{P}_{SOA}(\lambda)}{2}\left[1+(2r-1)\cos\left(-2\pi\frac{\lambda-\lambda_P}{\Delta\lambda_\tau}+\Phi_0\right)\right] \quad (3)$$

The modulation depth, or fringe depth, of $\tilde{P}_{DISC}^{CQP}(\lambda)$ is given by $\Delta\tilde{P}_{DISC}^{CQP}(\lambda) = r/(1-r)$, which is exactly equal to the ratio of ASE power emitted in the TE and TM polarization states. Figure 4(b) shows a comparison between the fringe depth and the directly measured TE/TM ASE ratio as a function of SOA bias current, which verifies the theoretical prediction above. The modest modulation of 0.6-0.8 dB, which is detailed in the inset for I = 150 mA, justifies the assumption of polarization independent ASE made in Section 2.

By comparing Fig. 4(a) to Fig. 2, it is observed that removing the polarizer at the SOA output simulates ASE emission from the SOA-based MZI or another switch in the same class. A key point of this paper is that the inline AMZI creates a fringe pattern and performs in-band ASE filtering, *only* if the ASE is polarized, which emphasizes the importance of including the polarizer in inline implementations of the DISC and UNI. This is different from an AMZI implemented with physically separated arms, which ideally transfers TE and TM polarized ASE components identically, and thus creates in-band filtering regardless of the presence of a polarizer. It should be noted that the polarizer has no impact on the probe signal as long as the polarization state at the output of the SOA remains fixed. This is generally satisfied when the input is aligned to a principal axis of the SOA, since this eliminates the effect of saturation-induced nonlinear polarization rotation [7]. Recalculating the IBSR obtained by including the polarizer at the AMZI input, taking the polarization dependence in Eq. (3) into account, we find that for $\Delta\lambda_F = \Delta\lambda_\tau$, $IBSR = r^{-1}$ for a TE-aligned probe signal and polarizer and $IBSR = (1-r)^{-1}$ for the TM case. This means that for a TE ASE fraction *r* slightly larger than 0.5, the *IBSR* becomes slightly smaller or larger than 3 dB when the signal polarization is aligned to TE or TM, respectively. This is clearly observed in Fig. 4(a), where r = 0.54 (0.78 dB).

The impact of in-band ASE filtering on the probe spectrum was investigated for input control pulse energy of 71 fJ at 25 GHz, a TE-aligned input CW probe power of -20.6 dBm, and an SOA bias current of 150 mA. The input probe power of -20.6 dBm is below the input saturation power of the SOA, and in this regime the ASE power available for the AMZI to suppress is maximum, which makes the impact of the in-band ASE filtering readily observable on an OSA. Fig. 5 shows a comparison between optical spectra, measured for I = 150 mA in 0.1 nm resolution, observed *with* the input polarizer (thick, solid) and *without* the polarizer (thin, dashed) for a phase bias of $\Phi_0 = 0.90\pi$, which provided the highest extinction ratio of the switched pulses. As expected, the ASE suppression across the center of the probe spectrum is very clear, and amounts to up to 17 dB in the present case. The filtering did not have an observable impact on the cross correlation trace, shown in the inset of Fig. 5 for the case including the polarizer, due to the averaging effect of the cross-correlation. Estimating the IBSR from the spectra in Fig. 5 we find IBSR = 2.7 dB, which is in excellent agreement with the theoretical prediction of $(0.54)^{-1} = 2.68\,dB$.

#7331 - $15.00 USD Received 3 May 2005; revised 13 June 2005; accepted 19 June 2005
(C) 2005 OSA

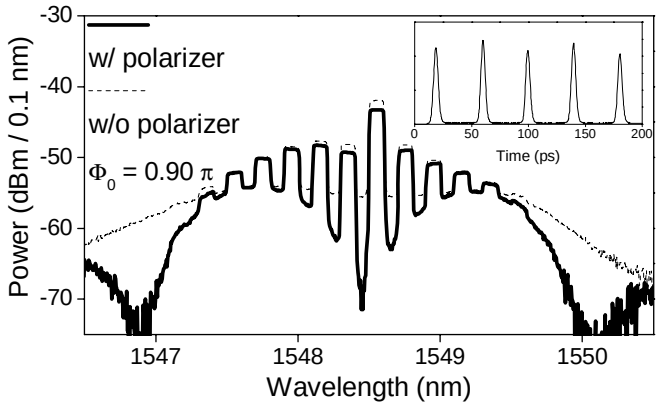

Fig. 5. Optical probe spectra at DISC output with input polarizer (thick, solid) and without polarizer (thin, dashed) for an SOA bias of 150 mA and an AMZI phase bias of $\Phi_0 = 0.90\ \pi$. Inset: Cross-correlation trace of switched probe.

4. Summary

In summary, we have theoretically identified a fundamental difference in the ASE suppression properties of all-optical high-speed switches based on SOAs, which allows us to divide such switches into two classes. One class of switches, which includes the DISC and UNI configurations, is found to be superior to the other class, which includes e.g. the SOA-based MZI and the TOAD switches, in the sense that these switches are expected to suppress the total in-band ASE power emitted by the SOAs by a factor of at least 3 dB. We demonstrate that the ASE emission of both switch classes can be investigated experimentally using a single hybrid DISC setup, simply by including or omitting a polarizer at the SOA output. A total ASE suppression of 2.7 dB in the signal bandwidth, and up to 17 dB in the center of the spectrum, was measured. We conclude that hybrid implementations of DISC and UNI configurations should include a polarizer at the SOA output to obtain in-band ASE suppression.

#7331 - $15.00 USD Received 3 May 2005; revised 13 June 2005; accepted 19 June 2005
(C) 2005 OSA